KI REPORTS
KIReports.org
TRANSLATIONAL RESEARCH

High-Throughput Splicing Assays Identify Known and Novel *WT1* Exon 9 Variants in Nephrotic Syndrome

Cathy Smith[1,2], Bala Bharathi Burugula[1], Ian Dunn[1], Swaroop Aradhya[3], Jacob O. Kitzman[1,2] and Jennifer Lai Yee[4]

[1]Department of Human Genetics, University of Michigan Medical School, Ann Arbor, Michigan, USA; [2]Department of Computational Medicine and Bioinformatics, University of Michigan Medical School, Ann Arbor, Michigan, USA; [3]Invitae, San Francisco, California, USA; and [4]Department of Pediatrics, Division of Nephrology, University of Michigan, Ann Arbor, Michigan, USA

Introduction: Frasier syndrome (FS) is a rare Mendelian form of nephrotic syndrome (NS) caused by variants which disrupt the proper splicing of *WT1.* This key transcription factor gene is alternatively spliced at exon 9 to produce 2 isoforms ("KTS+" and "KTS−"), which are normally expressed in the kidney at a ∼2:1 (KTS+:KTS−) ratio. FS results from variants that reduce this ratio by disrupting the splice donor of the KTS+ isoform. FS is extremely rare, and it is unclear whether any variants beyond the 8 already known could cause FS.

Methods: To prospectively identify other splicing-disruptive variants, we leveraged a massively parallel splicing assay. We tested every possible single nucleotide variant ($n = 519$) in and around *WT1* exon 9 for effects upon exon inclusion and KTS+/− ratio.

Results: Splice disruptive variants (SDVs) made up 11% of the tested point variants overall and were tightly concentrated near the canonical acceptor and the KTS+/− alternate donors. Our map successfully identified all 8 known FS or focal segmental glomerulosclerosis (FSGS) variants and 16 additional novel variants which were comparably disruptive to these known pathogenic variants. We also identified 19 variants that, conversely, increased the KTS+/KTS− ratio, of which 2 are observed in unrelated individuals with 46,XX ovotesticular disorder of sex development (46,XX OTDSD).

Conclusion: This splicing effect map can serve as functional evidence to guide the clinical interpretation of newly observed variants in and around *WT1* exon 9.

Kidney Int Rep (2023) **8,** 2117–2125; https://doi.org/10.1016/j.ekir.2023.07.033
KEYWORDS: differences in sex development; Frasier syndrome; focal segmental glomerulosclerosis; minigene splicing assay; nephrotic syndrome; *WT1* gene

Variants that disrupt proper pre-mRNA splicing contribute a share of the pathogenic burden in Mendelian forms of NS. One NS gene sensitive to splicing disruption is *WT1,* which encodes a key genitourinary transcription factor essential for podocyte development and integrity. Its disruption results in a phenotypic spectrum, including isolated NS, syndromic NS with tumors and gonadal dysgenesis, differences of sexual development, Wilms tumor, and leukemia.[1]

WT1 undergoes alternative splicing, including in exon 9 at a pair of donors which result in protein isoforms that differ by the 3 amino acids, KTS. These isoforms have overlapping and distinct functional roles: both act as transcription factors[2] but with partially different sequence motif specificities and gene targets.[3–6] Normally, they are expressed in the mature kidney[7,8] at a ∼2:1 ratio (KTS+:KTS−). Variants which disrupt the KTS+ donor reduce this ratio and cause an extremely rare syndrome called FS, consisting of male gonadal dysgenesis, NS, Wilms tumor, or gonadoblastoma (Figure 1a).[7–9]

Currently, 8 variants downstream of the KTS+ splice donor are known to cause FS or FSGS.[8–13] It remains unclear if other nearby variants are similarly splice

Correspondence: Jennifer Lai Yee, Department of Pediatrics, Division of Nephrology, University of Michigan, C.S. Mott Children's Hospital Room 12-250, 1540 East Hospital Drive, Ann Arbor, Michigan, USA. E-mail: chunlai@med.umich.edu; or Jacob O. Kitzman, Department of Human Genetics, University of Michigan Medical School, 4811 Med Sci II, 1241 E. Catherine St, Ann Arbor, Michigan, USA. E-mail: kitzmanj@umich.edu

Received 9 June 2023; accepted 31 July 2023; published online 5 August 2023

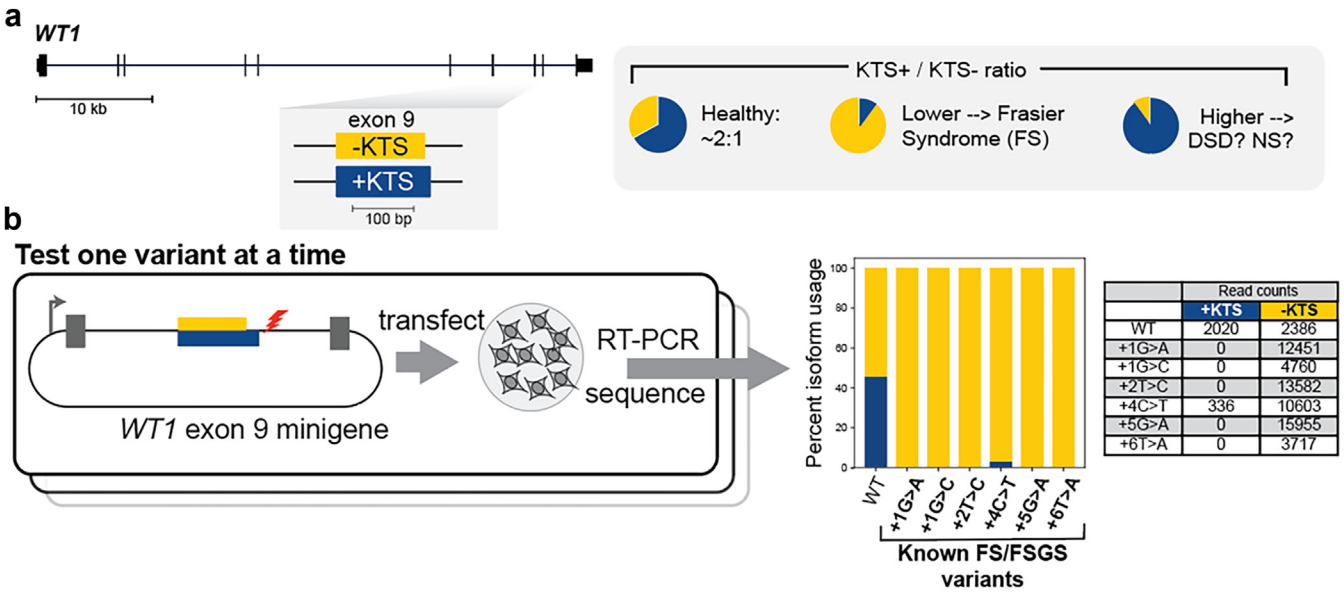

Figure 1. Alternative splicing with the known spliceogenic variant from the minigene assay. (a) *WT1* exon 9 alternative splice forms KTS+ (blue) and KTS− (yellow). (b) Six known Frasier or Focal segmental glomerulosclerosis syndrome variants tested individually by minigene assays followed by sequencing, with the percent of spliced reads from each isoform shown. DSD, differences of sex development; NS, nephrotic syndrome; RT-PCR, reverse transcriptase polymerase chain reaction.

disruptive. Accurate computational prediction of variants' splicing effects remains challenging, so we devised a massively parallel splice assay[14] to measure the splicing effects of every possible single nucleotide variant (SNV) in or near *WT1* exon 9 and the flanking introns ($N = 519$ variants). This identified all 8 known FS/FSGS variants and nominated an additional 49 *WT1* SNVs as splice disruptive, including 2 patient variants with uncertain interpretations (Table 2). This splicing effect map can support clinical interpretation of novel *WT1* variants and improve the accuracy of genetic diagnosis.

METHODS

Cell Culture

HEK293T and COS-7 cells were obtained from American Type Culture Collection and cultured in Dulbecco's modified Eagle's medium with high glucose, L-glutamine and sodium pyruvate (DMEM; GIBCO, Grand Island, NY) containing 10% fetal bovine serum and 1% penicillin-streptomycin (10,000 U/ml) (GIBCO). Media was checked monthly for mycoplasma contamination by polymerase chain reaction (PCR).

Saturation Mutagenesis Library Construction

A *WT1* minigene construct was prepared by cloning a fragment with *WT1* exon 9 plus 414 bp of its flanking introns into the vector pSPL3 (Invitrogen, Carlsbad, CA) at the BamHI site, an intronic context flanked by a synthetic first and last exon. This construct was subjected to saturation mutagenesis as previously described,[14] targeting the full exon +/− 40 bp (173 bp). Briefly, a mutant oligonucleotide pool was designed in which each position across the targeted region was successively replaced by 3 other mutant bases. The pool was synthesized by Twist Biosciences (South San Francisco, CA), amplified by limited-cycle PCR, and cloned by HiFi Assembly (New England Biolabs, Ipswitch, MA) into the vector backbone linearized by inverse PCR.

Mutant Plasmid Barcoding

A library of random 20mer barcode sequences were synthesized by Integrated DNA Technologies (Coralville, IA) and cloned into the downstream 3′ UTR at the MscI site by HiFi Assembly. The resulting pools of mutant *WT1* exon 9 minigenes with barcodes were transformed by electroporation into NEB 10-b *E. coli*, reaching library complexity of hundreds of barcoded clones per designed mutation. To enumerate the 3′UTR barcodes and identify the specific variant paired with each barcode, subassembly sequencing libraries were generated as previously described.[14,15]

Minigene Library Transfection

Mutant minigene libraries were transiently transfected into HEK293T (8 replicates) and COS-7 cells (2 replicates). At 24 hours post-transfection, cells were lysed by addition of Trizol and total RNA was purified with Direct-zol RNA Miniprep Kits (Zymo Research, Irvine, CA). A total of 3 to 5 µg total RNA was reverse transcribed using SuperScript III First-Strand Synthesis kit (Invitrogen) with oligo(dT) 20 primer following the

manufacturer's protocol. Afterwards, spliced transcript was amplified via seminested PCR using outer primer pairs, first SD6 forward (5′-TCTGAGTCACCTGGACAACC-3′) and SA2 reverse (5′-ATCTCAGTGGTATTTGTGAGC-3′), and inner primer pairs, JKlab232 (5′-AGTGAACTGCACTGTGACAAGCTGC) and SA2 reverse. Indexed illumina sequencing adaptors were added by PCR and the resulting RNA-seq libraries were submitted for paired-end 150-bp sequencing on Illumina HiSeq or NovaSeq instruments.

RNA-seq Processing and Splice Disruption Calling

RNA-seq reads were processed as previously described.[14] Briefly, reads containing plasmid barcodes were selected with cutadapt[16]; barcodes were clustered with starcode[17] and filtered to retain only those associated with a single-base variant. The paired, splice-informative read was aligned to the reference minigene sequence with the splice-aware read aligner STAR.[18] Custom python scripts (https://github.com/kitzmanlab/wt1_splice) were used to identify the isoform corresponding to each read: KTS+ (42.6% of all reads), KTS− (37.4%), exon 9 skipping ("SKIP," 19.1%), or all other isoforms ("OTHER"; collectively, <1% of all reads). The count of reads matching each isoform was tallied per barcode, then aggregated into a per-variant, per-isoform percent by taking a read-count weighted mean of the respective percentages across the associated barcodes.

To test the significance of splice disruption, we created for each variant a null distribution by bootstrap sampling a matching number of barcodes associated with intronic variants >10 bp outside the exon boundaries. Using this null distribution, we computed z scores for the observed per-isoform usage, then used Stouffer's method to aggregate z scores across replicates. SDVs were defined as those that were (i) significant at the $P < 0.05$ level (after Bonferroni correction for multiple testing), and either (ii) had either SKIP or OTHER usage at least 20% higher than the null, or (iii) an isoform log-ratio (calculated as log2[KTS+/KTS−]) of ≥1.5 or ≤ −1. Variants were defined as intermediate if they (i) passed the same significance test and had either (ii) SKIP or OTHER usage at least 10% higher than the null, or (iii) an isoform log-ratio of ≥ 1 or ≤ −0.5. Results were highly correlated across replicates; all SDVs were also called disruptive, at least half of the replicates when processed individually.

Prediction of Splice Site Strength

MaxEntScan scores[19] for variants at the common *WT1* exon 9 acceptor, KTS− donor, and KTS+ donor were computed using the maxentpy python module (https://github.com/kepbod/maxentpy). We first computed the splice site strength for the wild-type and mutant sequences for each and took the signed difference between the variant and wild-type scores.

Clinical Variant Interpretation

Deidentified clinical information was obtained for carriers of *WT1* exon 9 or flanking intron variants as identified in the course of clinical exome sequencing by Invitae. Deidentified data were provided with institutional review board approval (WCG IRB protocol #1167406).

RESULTS

Massively Parallel Splicing Assay for *WT1* Exon 9

To systematically identify SDVs, we established a minigene assay with *WT1* exon 9 and flanking introns (~200 bp on either side). We first individually tested the wild-type sequence and 6 pathogenic variants near the KTS+ donor known to cause FS or FSGS (Table 1). The wild-type construct showed a roughly even balance between the 2 isoforms (1:1.2 KTS+:KTS− ratio), whereas each of the known pathogenic variants abolished KTS+ usage (Figure 1b; Supplementary Figure S1). Therefore, consistent with previous reports,[20] minigenes can faithfully model *WT1* splicing defects associated with FS and FSGS.

We next set out to test the splicing effects of every possible SNV in and around *WT1* exon 9 (Figure 2a). We applied saturation mutagenesis to create a library of all possible SNVs in the exon and for 40 bp into each flanking intron. The mutant library was tagged with random 20mers in the 3′UTR to serve as barcodes allowing for the splicing effect of each mutation to be tracked. Nearly every possible SNV was represented (518/519; 99.8%) with a high degree of internal replication (mean = 79.7 barcodes per variant; Supplementary Figure S2).

We transfected HEK293T cells with the mutant minigene library pool and deeply sequenced the resulting spliced RNAs to quantify, for each mutation, the use of the KTS+ and KTS− isoforms, exon skipping ("SKIP") or all other splicing outcomes ("OTHER").

Table 1. Known splicing disruptive and disease-causing variants in WT1 exon 9 splicing donor site (IVS ds) +1 to +6

Variant	Reported disease	Previous experimental evidence of disruptive splicing
IVS9 ds+1 G>A	Frasier syndrome	
IVS9 ds+1 G>C	FSGS	
IVS9 ds+2 T>C	Frasier syndrome	Loss of +KTS isoform in minigene assay and in homozygous mouse embryos
IVS9 ds+4 C>T	Frasier syndrome	Loss of +KTS isoform in minigene assay
IVS9 ds+5 G>A	Frasier syndrome	Loss of +KTS isoform in minigene assay
IVS9 ds+6 T>A	Frasier syndrome	

FSGS, focal segmental glomerulosclerosis.

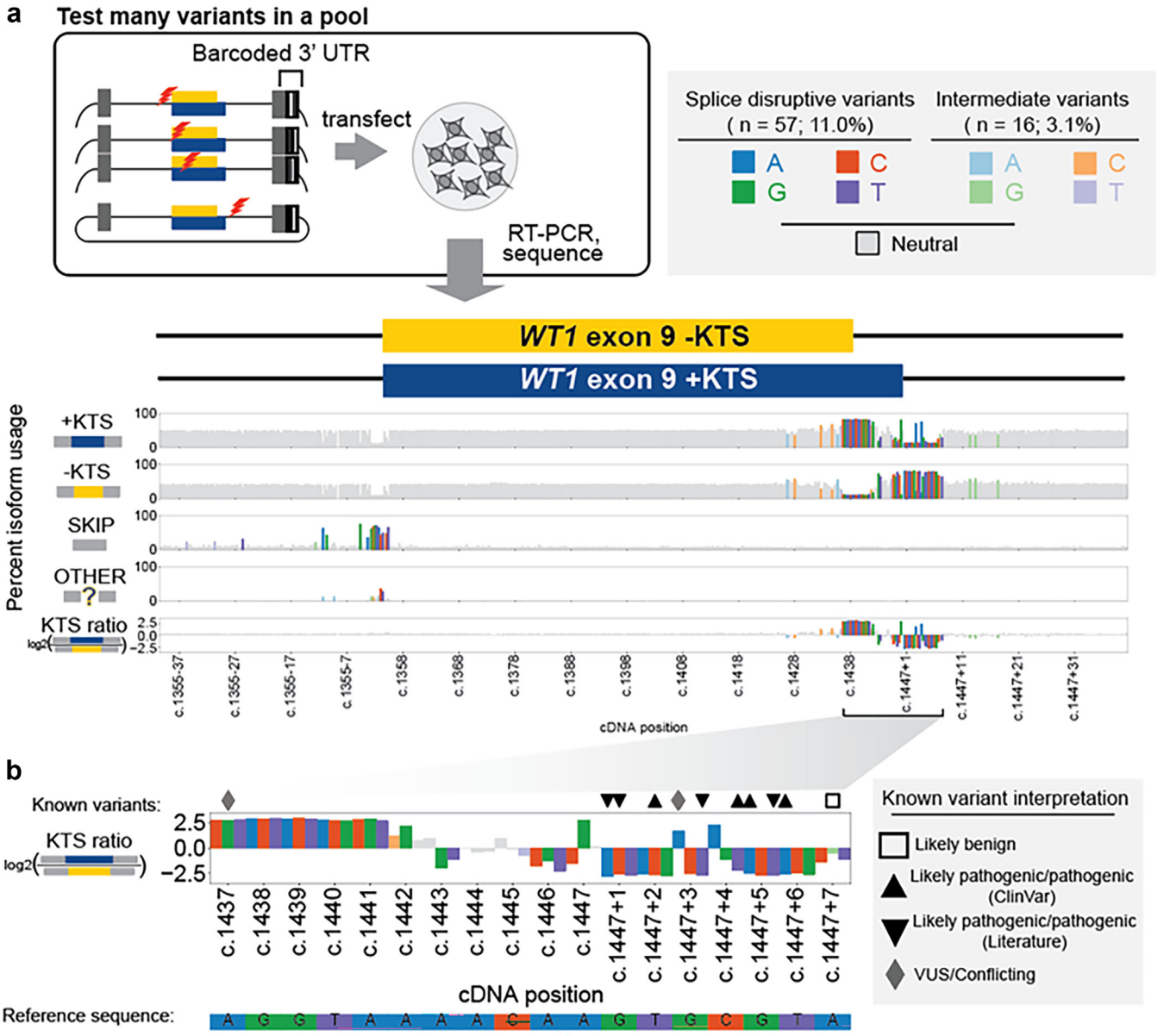

Figure 2. Screening for all possible splice-disruptive variants in *WT1* exon 9. (a) Splicing effect map for all 518 single-nucleotide variants in/around *WT1* exon 9 from a massively parallel splice assay. Each bar represents a single variant plotted by its cDNA position (x-axis), with dark shading for splice disruptive variants, light shading for intermediate ones, and gray for variants with no effect upon splicing. The first 4 tracks show the percent usage of KTS+, KTS−, SKIP, and OTHER isoforms. Final y-axis track shows the log2(KTS+/KTS−) ratio. (b) Zoom to the alternative donors showing KTS+/KTS− ratio and reference sequence. Known variants are shown above the plot with symbols denoting existing interpretation.

Mutations' effects upon isoform usage were reproducible within the HEK293T biological replicates (median pairwise Pearson's $r = 0.94$) and between HEK293T replicates and a second cell line, COS-7 (median between cell line pairwise Pearson's $r = 0.93$; Supplementary Figure S3).

The resulting map shows that, as expected, sensitivity to splicing disruption is heavily concentrated near the canonical splice sites, in particular the alternate KTS+ and KTS− donors (Figure 2b). Overall, of the 518 measured SNVs, only 57 (11.0%) altered splicing with an additional 16 (3.1%) having an intermediate effect on splicing (Table 2; Supplementary Table S1). Of the disruptive variants, all but 1 were near (+/− 15 bp) either the splice acceptor or one of the donors, consistent with disruption of those sites' consensus motifs. The primary disruptive effect for most variants (43/57; 75.4%) was to alter the KTS+/KTS− ratio, with the direction of effect roughly evenly split between shifting the balance toward KTS− and KTS+ (24 variants and 19 variants, respectively). A minority of variants led to complete exon skipping ($n = 14$) or activated a cryptic acceptor 17 bp downstream of the native one ($n = 2$), each of which would yield

Table 2. Splice assay scores for previously reported pathogenic variants for Frasier Syndrome, focal segmental glomerulosclerosis, or 46,XX OTDSD

Variant	Genomic position (hg19)	Splice score log2 (KTS+/KTS−)	Called splice disruptive?	ClinVar interpretation	Literature report as pathogenic	Variant consequence
c.1437A>G	32413528	2.76	Yes	Conflicting interpretations	Yes	Synonymous
c.1447+1G>A	32413517	−2.81	Yes		Yes	Intronic
c.1447+1G>C	32413517	−2.56	Yes		Yes	Intronic
c.1447+2T>C	32413516	−2.64	Yes	Likely pathogenic	Yes	Intronic
c.1447+3G>A	32413515	1.72	Yes	Uncertain significance	This study	Intronic
c.1447+3G>T	32413515	−2.71	Yes		Yes	Intronic
c.1447+4C>T	32413514	−2.21	Yes	Pathogenic/Likely pathogenic	Yes	Intronic
c.1447+5G>A	32413513	−2.51	Yes	Pathogenic	Yes	Intronic
c.1447+5G>T	32413513	−2.69	Yes		Yes	Intronic
c.1447+6T>A	32413512	−2.58	Yes	Pathogenic	Yes	Intronic

frameshifted transcript predicted to undergo nonsense mediated decay.

Identification of Known and Novel Variants Disrupting KTS+ Usage

We focused first on the 8 known FS/FSGS variants as described in the ClinVar database[21] or published case reports.[8–13] All 8 dramatically lowered the KTS+:KTS− balance, as quantified by log2(KTS+/KTS−) scores well below 0 (all ≤ −2.21; Figure 2b; Figure 3; Table 2). In contrast, of the 19 variants listed in ClinVar with an interpretation of Likely Benign, our assay scored 18 as neutral, with 1 (c.1447+7A>G) barely meeting the threshold for intermediate score range (score: −0.52), for which the *in vivo* impact is unclear as clinical information was unavailable. Therefore, pooled minigene assays can effectively discriminate between known pathogenic SDVs and neutral polymorphisms.

We next asked whether this map could prospectively identify as-yet unreported variants which disrupt KTS+. We identified 16 additional SDVs which disrupted KTS+ comparably to the known FS/FSGS variants (median log2 ratio score: −2.14; Supplementary Table S1), most of which were corroborated by splice site strength predictions from MaxEntScan (median MaxEntScan score = −2.40; Supplementary Figure S4).[19] Among these, 6 were located within the codon region specific to the KTS+ isoform; 4 of these were synonymous variants, which as a class may be overlooked during classification. None of these is yet deposited in ClinVar or in published reports; however, but based on their disruptiveness in this assay, they represent potential novel pathogenic variants.

Other Splice Disruptive Outcomes

Finally, we searched this map for variants that disrupt splicing in other ways and identified 19 variants that increased the KTS+/− ratio, opposite the effect associated with FS (Figure 2b; Figure 3). Notably, 2 have been observed in patients with 46,XX ovotesticular differences in sexual development (46,XX OTDSD). The first, c.1437A>G, is a synonymous variant recently reported[22] as a *de novo* mutation in a patient with 46,XX OTDSD. Consistent with the strong shift toward KTS+ in our map (score: 2.76), it is predicted by MaxEntScan to weaken the KTS− donor 2 bases downstream (Supplementary Figure S4). We observed similar effects from an additional 17 variants near the KTS− donor (median log2 ratio score: 2.83, range: 2.20–2.98). Another variant, c.1447+3G>A (log2 ratio score: 1.72), downstream of the KTS+ donor, was observed during clinical exome sequencing in a proband (age range: 10–15 y) with 46,XX OTDSD. Notably, no renal abnormalities or a history of Wilms tumor was reported for either of these 2 individuals. In contrast to the variants near the KTS− donor, this and one other variant not yet observed clinically (c.1447+4C>A) are predicted to strengthen the KTS+ donor (Supplementary Figure S4), possibly leading it to outcompete its upstream counterpart. Finally, we identified a cluster of 14 variants within 26 bp of the *WT1* acceptor which led to complete skipping of exon 9, or use of an alternate cryptic acceptors, in each case leading a frameshift and premature truncation (Figure 2a; Supplementary Table S1). None of those variants are yet reported in ClinVar or population databases.

SDV Depletion Among Population Rare Variants

We next intersected these measurements with gnomAD, a population database of variation from whole exome and genome sequencing of cohorts depleted for severe early-onset genetic disorders.[23] Of the *WT1* variants measured in this splicing screen, 30 were found in gnomAD (18 intronic, 12 exonic), all of which were rare (allele frequency less than 10^{-4}). Notably, among these, a stop-gain variant (c.1387C>T; p.Arg463Ter) classified as pathogenic in ClinVar was found in 1 individual in gnomAD, consistent with incomplete penetrance and nonzero prevalence of

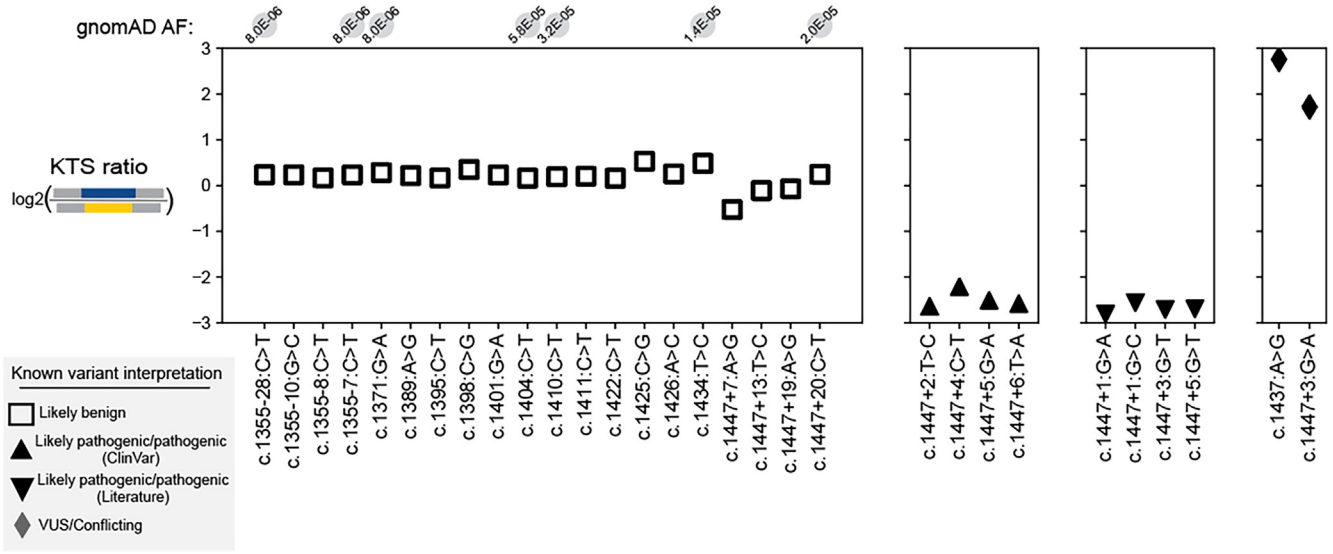

Figure 3. Correlation between the splicing effect from minigene assay and pathogenicity in variant-phenotype database. KTS+/KTS− ratios for variants reported in the literature or in ClinVar, grouped by interpretation, with population allele frequency shown above the plot for variants present in gnomAD.

genetic disorders such as NS or Wilms Tumor in "healthy" population databases. The remaining 29 gnomAD variants were all measured as splice neutral in our screen (Supplementary Table S1; Figure 3), a significant depletion compared to random expectation (Fisher exact $P < 0.05$), consistent with selection against *WT1* exon 9 splice disruption among the general population.

DISCUSSION

Here, we applied a massively parallel splicing assay to systematically test the effects of every single-nucleotide variant in and near *WT1* exon 9, a hotspot for multiple genetic forms of NS including FS. The resulting splicing effect map correctly identified all 7 known FS variants[8-11,13] as associated with reduced KTS+/KTS− ratio, along with another variant reported to cause isolated steroid resistant NS and FSGS.[12] In contrast, all 20 variants which appear in the ClinVar database with an interpretation of Likely Benign scored as splice neutral or intermediate, whereas rare population variants in the gnomAD database were exclusively splice-neutral. Therefore, this splicing assay was highly sensitive and specific for identification of pathogenic variants causing *WT1* exon 9 splice disruption.

FS is extremely rare: in all, fewer than 200 cases have been reported, represented by only 7 distinct FS variants.[8-11,13] Two of these 7 variants (at the +4 and +5 positions) account for most of the FS case reports to date: taking the count of ClinVar submissions as a proxy for frequency, c.1447+4C>T and c.1447+5G>A together had 24 records, compared with only 2 records combined across the 5 other known FS variants. The 2 recurrent variants overlap the only CpG dinucleotide in the KTS+ region, and their frequency is likely explained by the ~10-fold higher *de novo* mutation rate at germline-methylated CpGs.[24] Therefore, it is reasonable to expect that there may be a tail of additional variants which are rare even within the context of this rare disorder. Indeed, our results implicate an additional SNVs to be similarly decreasing the KTS+/KTS− ratio, and nominate these as new, as yet-unreported variants with the potential to cause FS/FSGS.

Our results highlight how different variants at the same or adjacent positions can have opposite functional and clinical impacts. Indeed, the entire KTS+/− donor region is perfectly conserved with no sequence changes among extant placental mammals,[25] which may signal its importance but does not distinguish individual variants' effects. As our splicing effect map shows, splicing disruption is both site-dependent and variant-dependent, with effects split approximately evenly between variants that shift the balance toward KTS+ versus those that shift it toward KTS−.

Our map also identified 19 variants, which increase the KTS+/KTS− ratio, either by weakening the KTS− donor or strengthening the KTS+ donor. One of these variants was previously reported[22] in an individual with 46,XX OTDSD, and we report an additional, unrelated patient with a similar presentation carrying a different variant. Converse to FS variants, which are associated with reduced *SRY* expression in male patients with FS[26] and mouse models,[27] these variants favoring KTS+ may lead to dysregulation or overactivation of *SRY*, the master regulator of male sex determination.[28] KTS+ and KTS− have partially

distinct activities, and nonidentical DNA binding targets, downstream transcriptomic signatures, and ultimately functional roles.[3,5,29] Although it is clear that variants that disrupt KTS+/KTS− ratio in either direction exert pathological effects on gonadal development and kidney function, further work is needed to define whether this is caused by the imbalance *per se* or both alleles' dosage sensitivity.

This study focused on the effects of variants in or near *WT1* exon 9 splicing donor sites. In some Mendelian disorders, missense or synonymous variants may alter splicing by disrupting regulatory elements beyond the canonical splice sites, termed exonic splice enhancers and silencers.[30] Such effects have been observed by other systematic splice assays[14] including at other *WT1* exons.[31] Here, though, we observed that variants to the interior of *WT1* exon 9 had little impact upon its splicing. This suggests that *WT1* exon 9 either does not depend on exonic splice regulatory elements for its definition, or that any such elements may be robust to perturbation by single nucleotide variants. In addition, variants at other loci beyond *WT1* can cause pathogenic perturbation of *WT1* KTS+/− ratio *in trans*. For example, insulin-like growth factor I upregulated *WT1* KTS− isoform in breast cancer, inflicting a poorer prognosis[32]; and mutation in another key kidney transcriptional factor, *LMX1B*, decreased the expression of KTS− and therefore disrupted KTS+/KTS−, resulting in FSGS with decreased expression in podocyte genes.[33] Future work is needed to systematically determine *trans* influences upon *WT1* splicing, and to include them as targets for genetic testing.

In addition to SDVs near the KTS+/− donors, we discovered variants that caused exon skipping or usage of out-of-frame acceptors; although to the best of our knowledge, none of those variants has been described in humans. Skipping of *WT1* exon 9 would yield an in-frame transcript lacking the third zinc finger domain, but the stability and function of the resulting protein has not yet been characterized. Chimeric transgenic mice heterozygous for a variant truncating ZF3 at codon 396 ($Wt1^{tmT396}$) recapitulate Denys-Drash Syndrome phenotypes including mesangial sclerosis, male genital defects, and Wilms tumor.[34] Our screen nominates those variants as deleterious, but it remains unclear what their clinical and phenotypic impact would be, or if they are compatible with life.

Further genotype-phenotype correlations with the *WT1* SDVs identified here will require continued expansion of exome and genome sequencing in individuals with NS. We screened several existing cohorts including Nephrotic Syndrome Study Network,[35] which is a large North American cohort consisting of patients with NS (approximately 600 individuals), the Clinical Phenotyping Resource and Biobank Core,[36] an independent North American cohort comprising patients with chronic kidney disease (around 200 individuals), and the Steroid Resistant Nephrotic Syndrome Study Group (~2000 unrelated, international families with steroid-resistant NS).[37] Among these cohorts, we did not identify patients with any of the observed novel SDVs, potentially reflecting the severity of their effects as well as the genetic heterogeneity of NS.

Our minigene splicing assay has certain limitations, including the limited sequence context (+/− 200 bp) included in the minigene construct and the use of a heterologous cell lines (HEK293-T and COS-7) in which the splice factor milieu may differ from that of the developing kidney. A mitigating factor is that the *WT1* KTS+/− ratio has previously been noted to be remarkably stable across different tissues *in vivo*, suggesting there is leeway in modeling it in culture.[27] Future experimental validation in more physiologically relevant systems (e.g., induced pluripotent stem cell-derived organoids[38] or animal models[27]) is needed to confirm variants' splice disruptive effects in the context of the full-length endogenous locus and investigate their downstream functional consequences. Nevertheless, the measured effects were highly consistent with standing clinical variants' interpretation. Given the gene-agnostic nature of this approach and its scalability, our study demonstrates the feasibility of massively parallel splice minigene assays to identify candidate SDVs more broadly in NS genes.

These results may be useful in interpreting variants found in individuals who do not display every feature of FS. For instance, variants disrupting KTS+ in karyotypically female individuals (46,XX) may lead to progressive glomerulopathy, but due to the lack of gonadal dysgenesis, FS may not be suspected and *WT1* genetic testing might not be pursued.[39] In conclusion, our systematic screen provides a lookup table of SDVs in *WT1* exon 9, circumventing the need for single variant minigene studies. The availability of functional evidence for newly observed rare variants can facilitate their resolution, lessening the burden of variant interpretation on clinicians, and shortening the diagnostic odyssey for patients with NS.

DISCLOSURE

SA is an employee of Invitae. JOK serves as a scientific advisor to MyOme, Inc. All the other authors have declared no competing interests.

ACKNOWLEDGMENTS

We would like to thank Ana Morales at Invitae for assistance with review of clinical records. We also would like to

express our sincere gratitude to our colleague, Damian Fermin at the University of Michigan, and our collaborations, Dr. Nina Mann and Dr. Friedhelm Hildebrandt at the Boston Children's Hospital, Harvard Medical School, to examine the observed novel splicing disruptive variants in patients from Nephrotic Syndrome Study Network/C-probe cohort study and from the international steroid resistant NS (SRNS) cohort study, respectively.

This work was supported by the National Institute of General Medical Sciences (R01GM129123 to JOK) and a National Institute of Child Health & Human Development Clinical Scientist Institutional Career Development Program Award (5K12HD028820 to JLY).

AUTHOR CONTRIBUTIONS

JOK and JLY devised the study. BB, ID, and JLY performed experiments. CS, JOK, and JLY analyzed the data. SA abstracted clinical information. CS, JLY, and JOK wrote the manuscript. All authors reviewed the manuscript prior to submission.

SUPPLEMENTARY MATERIAL

Supplementary File (PDF)

Figure S1. Sashimi plot from Integrative Genomics Viewer (IGV) showing read pileup and splice junction read counts from deep sequencing of RT-PCR products from each individual minigene assay.

Figure S2. Distinct barcode counts for each mutation (mean across replicates) by position.

Figure S3 Inter-replicate correlations of measured isoform use.

Figure S4. MaxEntScan predictions of splice site strength.

Table S1. Measured splicing effect, calls of disruptiveness, and additional information, for all tested variants in/near *WT1* exon 9.

REFERENCES

1. Mrowka C, Schedl A. Wilms' tumor suppressor gene WT1: from structure to renal pathophysiologic features. *J Am Soc Nephrol*. 2000;11(suppl 16):S106–S115. https://doi.org/10.1681/ASN.V11suppl_2s106
2. Larsson SH, Charlieu JP, Miyagawa K, et al. Subnuclear localization of WT1 in splicing or transcription factor domains is regulated by alternative splicing. *Cell*. 1995;81:391–401. https://doi.org/10.1016/0092-8674(95)90392-5
3. Bickmore WA, Oghene K, Little MH, Seawright A, van Heyningen V, Hastie ND. Modulation of DNA binding specificity by alternative splicing of the Wilms tumor wt1 gene transcript. *Science*. 1992;257:235–237. https://doi.org/10.1126/science.1321494
4. Wells J, Rivera MN, Kim WJ, Starbuck K, Haber DA. The predominant WT1 isoform (+KTS) encodes a DNA-binding protein targeting the planar cell polarity gene Scribble in renal podocytes. *Mol Cancer Res*. 2010;8:975–985. https://doi.org/10.1158/1541-7786.MCR-10-0033
5. Potluri S, Assi SA, Chin PS, et al. Isoform-specific and signaling-dependent propagation of acute myeloid leukemia by Wilms tumor 1. *Cell Rep*. 2021;35:109010. https://doi.org/10.1016/j.celrep.2021.109010
6. Lefebvre J, Clarkson M, Massa F, et al. Alternatively spliced isoforms of WT1 control podocyte-specific gene expression. *Kidney Int*. 2015;88:321–331. https://doi.org/10.1038/ki.2015.140
7. Klamt B, Koziell A, Poulat F, et al. Frasier syndrome is caused by defective alternative splicing of WT1 leading to an altered ratio of WT1 +/-KTS splice isoforms. *Hum Mol Genet*. 1998;7:709–714. https://doi.org/10.1093/hmg/7.4.709
8. Barbaux S, Niaudet P, Gubler MC, et al. Donor splice-site mutations in WT1 are responsible for Frasier syndrome. *Nat Genet*. 1997;17:467–470. https://doi.org/10.1038/ng1297-467
9. Kikuchi H, Takata A, Akasaka Y, et al. Do intronic mutations affecting splicing of WT1 exon 9 cause Frasier syndrome? *J Med Genet*. 1998;35:45–48. https://doi.org/10.1136/jmg.35.1.45
10. Tsuji Y, Yamamura T, Nagano C, et al. Systematic review of genotype-phenotype correlations in Frasier syndrome. *Kidney Int Rep*. 2021;6:2585–2593. https://doi.org/10.1016/j.ekir.2021.07.010
11. Miyoshi Y, Santo Y, Tachikawa K, et al. Lack of puberty despite elevated estradiol in a 46,XY phenotypic female with Frasier syndrome. *Endocr J*. 2006;53:371–376. https://doi.org/10.1507/endocrj.k05-180
12. Gast C, Pengelly RJ, Lyon M, et al. Collagen (COL4A) mutations are the most frequent mutations underlying adult focal segmental glomerulosclerosis. *Nephrol Dial Transplant*. 2016;31:961–970. https://doi.org/10.1093/ndt/gfv325
13. Bruening W, Bardeesy N, Silverman BL, et al. Germline intronic and exonic mutations in the Wilms' tumour gene (WT1) affecting urogenital development. *Nat Genet*. 1992;1:144–148. https://doi.org/10.1038/ng0592-144
14. Gergics P, Smith C, Bando H, et al. High-throughput splicing assays identify missense and silent splice-disruptive POU1F1 variants underlying pituitary hormone deficiency. *Am J Hum Genet*. 2021;108:1526–1539. https://doi.org/10.1016/j.ajhg.2021.06.013
15. Hiatt JB, Patwardhan RP, Turner EH, Lee C, Shendure J. Parallel, tag-directed assembly of locally derived short sequence reads. *Nat Methods*. 2010;7:119–122. https://doi.org/10.1038/nmeth.1416
16. Martin M. Cutadapt removes adapter sequences from high-throughput sequencing reads. *EMBnet J*. 2011;17:10–12. https://doi.org/10.14806/ej.17.1.200
17. Zorita E, Cusco P, Filion GJ. Starcode: sequence clustering based on all-pairs search. *Bioinformatics*. 2015;31:1913–1919. https://doi.org/10.1093/bioinformatics/btv053
18. Dobin A, Davis CA, Schlesinger F, et al. STAR: ultrafast universal RNA-seq aligner. *Bioinformatics*. 2013;29:15–21. https://doi.org/10.1093/bioinformatics/bts635
19. Yeo G, Burge CB. Maximum entropy modeling of short sequence motifs with applications to RNA splicing signals. *J Comput Biol*. 2004;11:377–394. https://doi.org/10.1089/1066527041410418
20. Yang C, Romaniuk PJ. The ratio of +/-KTS splice variants of the Wilms' tumour suppressor protein WT1 mRNA is determined by an intronic enhancer. *Biochem Cell Biol*. 2008;86:312–321. https://doi.org/10.1139/o08-075

21. Landrum MJ, Lee JM, Benson M, et al. ClinVar: improving access to variant interpretations and supporting evidence. *Nucleic Acids Res*. 2018;46:D1062–D1067. https://doi.org/10.1093/nar/gkx1153
22. Sirokha D, Gorodna O, Vitrenko Y, et al. A novel WT1 mutation identified in a 46,XX testicular/ovotesticular DSD patient results in the retention of Intron 9. *Biology (Basel)*. 2021;10:1248. https://doi.org/10.3390/biology10121248
23. Karczewski KJ, Francioli LC, Tiao G, et al. The mutational constraint spectrum quantified from variation in 141,456 humans. *Nature*. 2020;581:434–443. https://doi.org/10.1038/s41586-020-2308-7
24. Kong A, Frigge ML, Masson G, et al. Rate of de novo mutations and the importance of father's age to disease risk. *Nature*. 2012;488:471–475. https://doi.org/10.1038/nature11396
25. Sullivan PF, Meadows JRS, Gazal S, et al. Leveraging base-pair mammalian constraint to understand genetic variation and human disease. *Science*. 2023;380:eabn2937. https://doi.org/10.1126/science.abn2937
26. Schumacher V, Gueler B, Looijenga LH, et al. Characteristics of testicular dysgenesis syndrome and decreased expression of SRY and SOX9 in Frasier syndrome. *Mol Reprod Dev*. 2008;75:1484–1494. https://doi.org/10.1002/mrd.20889
27. Hammes A, Guo JK, Lutsch G, et al. Two splice variants of the Wilms' tumor 1 gene have distinct functions during sex determination and nephron formation. *Cell*. 2001;106:319–329. https://doi.org/10.1016/s0092-8674(01)00453-6
28. Miyamoto Y, Taniguchi H, Hamel F, Silversides DW, Viger RS. A GATA4/WT1 cooperation regulates transcription of genes required for mammalian sex determination and differentiation. *BMC Mol Biol*. 2008;9:44. https://doi.org/10.1186/1471-2199-9-44
29. Ullmark T, Montano G, Gullberg U. DNA and RNA binding by the Wilms' tumour gene 1 (WT1) protein +KTS and -KTS isoforms-From initial observations to recent global genomic analyses. *Eur J Haematol*. 2018;100:229–240. https://doi.org/10.1111/ejh.13010
30. Rossanti R, Horinouchi T, Yamamura T, et al. Evaluation of suspected autosomal Alport syndrome synonymous variants. *Kidney360*. 2022;3:497–505. https://doi.org/10.34067/KID.0005252021
31. Ke S, Anquetil V, Zamalloa JR, et al. Saturation mutagenesis reveals manifold determinants of exon definition. *Genome Res*. 2018;28:11–24. https://doi.org/10.1101/gr.219683.116
32. Tuna M, Itamochi H. Insulin-like growth factor I regulates the expression of isoforms of Wilms' tumor 1 gene in breast cancer. *Tumori*. 2013;99:715–722. https://doi.org/10.1177/030089161309900612
33. Hall G, Lane B, Chryst-Ladd M, et al. Dysregulation of WTI (-KTS) is associated with the kidney-specific effects of the LMX1B R246Q mutation. *Sci Rep*. 2017;7:39933. https://doi.org/10.1038/srep39933
34. Patek CE, Little MH, Fleming S, et al. A zinc finger truncation of murine WT1 results in the characteristic urogenital abnormalities of Denys-Drash syndrome. *Proc Natl Acad Sci U S A*. 1999;96:2931–2936. https://doi.org/10.1073/pnas.96.6.2931
35. Gadegbeku CA, Gipson DS, Holzman LB, et al. Design of the nephrotic syndrome Study Network (Neptune) to evaluate primary glomerular nephropathy by a multidisciplinary approach. *Kidney Int*. 2013;83:749–756. https://doi.org/10.1038/ki.2012.428
36. Troost JP, Hawkins J, Jenkins DR, et al. Consent for genetic biobanking in a diverse multisite CKD cohort. *Kidney Int Rep*. 2018;3:1267–1275. https://doi.org/10.1016/j.ekir.2018.06.002
37. Sadowski CE, Lovric S, Ashraf S, et al. A single-gene cause in 29.5% of cases of steroid-resistant nephrotic syndrome. *J Am Soc Nephrol*. 2015;26:1279–1289. https://doi.org/10.1681/ASN.2014050489
38. Harder JL, Menon R, Otto EA, et al. Organoid single cell profiling identifies a transcriptional signature of glomerular disease. *JCI Insight*. 2019;4:e122697. https://doi.org/10.1172/jci.insight.122697
39. Demmer L, Primack W, Loik V, Brown R, Therville N, McElreavey K. Frasier syndrome: a cause of focal segmental glomerulosclerosis in a 46,XX female. *J Am Soc Nephrol*. 1999;10:2215–2218. https://doi.org/10.1681/ASN.V10102215